SUPPLEMENTARY DATA

Supplementary experimental procedures

AICAR tolerance test
LKB1 MKO and WT mice were fasted for 11 hours prior to the AICAR tolerance test. Mice were randomized and the test was performed blinded. Mice received AICAR (0.5g kg^{-1} body wt) by intraperitoneal injection. Blood was collected from the tail vein and blood glucose concentration was measured via a glucometer (Contour, Bayer Health Care, Germany).

Treadmill exercise test
Prior to the treadmill exercise test, all mice were acclimatized on a treadmill with electric shockers. Acclimatization was done for 3 days with 2 days rest prior to testing day. Acclimatization consisted of 2 min at rest in the treadmill apparatus (TSE Systems GmbH, Germany) followed by running at 0% incline: Day 1) 5 min at 10 m/min and 5 min at 14 m/min, Day 2) 5 min at 14 m/min and 5 min at 17 m/min, Day 3) 10 min at 17 m/min. The maximal running speed test was performed blinded and the mice started at 10.8 m/min and increased by 2.4 m/min every 2nd min until the mice were unable to keep up with the treadmill. Cut-off speed was defined as the maximal running speed.

Measurement of respiratory exchange ratio and oxygen uptake at rest and during treadmill exercise
For recording during rest, mice were acclimatized to individual cages for 24 hours prior to measurement. The mice were allowed access to chow food and water ad libitum at all times while housed in individual cages. Immediately prior to recording, the cages were sealed and O_2 uptake and CO_2 production were measured for 24h using a CaloSys apparatus (TSE Systems GmbH, Germany). The respiratory exchange ratio (RER) was calculated as VCO_2 production/VO_2 uptake. For recording during exercise the mice were rested for two to four days after the treadmill exercise test. Subsequently LKB1 MKO and WT mice were run for 24 min on the treadmill. The LKB1 MKO mice were assigned to run at 60% (12.5 m/min) of their maximal running speed, whereas WT mice were randomized to run at either 30% (12.5 m/min) or 60% (25 m/min) of their maximal running speed. AMPKα2 and respective WT mice were exercised at 50% of their maximal running speed, corresponding to 13m/min and 18m/min, respectively. During the exercise bout O_2 uptake and CO_2 production were measured and RER was calculated as VCO_2 production/VO_2 uptake. %CHO use was calculated as (RER-0.7)/0.3 and %FAT use as (100%-%CHO). CHO utilization was calculated as ((20kJ/L • VO_2 uptake) • %CHO) and FAT utilization was calculated as ((20kJ/L • VO_2 uptake) • %FAT).

Fatty acid oxidation in isolated muscle
LKB1 MKO and WT mice were anaesthetized with sodium pentobarbital (6 mg $100g^{-1}$ body wt) and *extensor digitorum longus* (EDL) muscles were carefully dissected tendon to tendon for muscle incubations. Fatty acid (FA) metabolism experiments were conducted using procedures described previously (1;2). Isolated EDL muscles were placed in warmed ($30^{O}C$) Krebs-Henseleit Ringer buffer pH 7.4 containing 2 mM pyruvate, 2% fatty acid free BSA and 0.5 mM palmitic acid. Palmitic acid was dissolved in ethanol and a small volume was added to the buffer (<1% total buffer volume) to achieve the desired palmitate concentration. The proximal and distal tendons of isolated EDL muscles were tied with silk suture and mounted to a force transducer in a 15 ml incubation reservoir (Radnoti, CA, USA). After an initial incubation of 20 min at resting tension (4-5 mN), the incubation buffer was replaced with the same buffer described above supplemented with 0.5 μCi/ml of [1-^{14}C] palmitate (Amersham BioSciences, UK). FA oxidation was measured in resting or contracting EDL muscle (50 Hz, 350 ms pulse duration, 6 tetani min^{-1}) over 25 min. At the completion of the contraction protocol muscles were removed and snap-frozen in liquid nitrogen and stored at $-80^{O}C$. The incubation medium was collected and gaseous $^{14}CO_2$ was liberated with 1 M acetic acid and trapped with vials containing 0.4 ml

benzethonium hydroxide. Radioactivity in trapped $^{14}CO_2$ was determined by liquid scintillation counting using Ultima Gold (Perkin Elmer, MA, USA). Frozen muscle strips were quickly weighed, homogenized in 2:1 chloroform:methanol and 750 µl of the aqueous phase was subjected to liquid scintillation counting. Counts obtained within the aqueous phase were combined with the counts from trapped $^{14}CO_2$ to calculate rates of FA oxidation.

Glucose transport in isolated muscle

LKB1 MKO and WT mice were anesthetized by sodium pentobarbital (6 mg $100g^{-1}$ body wt). EDL muscles were quickly excised and suspended by ligatures at resting tension (4-5 mN) in incubation chambers (Multi Myograph system; Danish Myo-Technology, Aarhus, Denmark). The muscles were incubated in a pre-buffer (Krebs-Henseleit-Ringer buffer with addition of 8 mM Mannitol, 2 mM pyruvate, and 0.1% BSA) 40 min at 30°C and oxygenated with a gas mixture containing 95% O_2 and 5% CO_2, as previously described (3). After pre-incubation muscles were stimulated electrically to contract for 10 min (moderate protocol: 2s/15s, 0.2 ms pulses, 100 Hz, 40 V; intense protocol: 10s/30s, 0.1 ms pulses, 100 Hz, 100 V). 2-Deoxyglucose (2-DG) uptake was measured for 10 min either during stimulation (moderate protocol) or immediately after stimulation (intense protocol). Pilot studies indicated that in this mouse model no differences were obtained whether 2-DG uptake was measured during or immediately after stimulation in the intense stimulation protocol. The choice to measure after stimulation in the intense protocol was made to completely simulate conditions used by Koh et al. (4).

Glucose clearance during in vivo exercise

On the experimental day mice fasted for ~2h were randomized to either the resting or the exercising group. Immediately before the start of the rest/exercise period, mice were given an intraperitoneal injection with a bolus of saline (800 µl/100 g body wt) containing 0.1 mM 2-deoxyglucose and 60 µCi/ml 2-[^{3}H]deoxyglucose corresponding to ~12 µCi/mouse as previously described (5). WT mice were assigned to run at either 30% (12.5 m/min) or 60% (25 m/min) of their maximal running speed for 20 min, whereas LKB1 MKO mice were assigned to run at 60% (12.5 m/min) of their maximal running speed for 20 min. Resting mice were placed in a treadmill lane which was turned off. Immediately before and during exercise/rest, mice were quickly removed from the treadmill (<1 min) at time points –2, 10, and 20 min to collect tail blood (~30 µl). Plasma glucose concentration was determined by a glucometer (Contour, Bayer Health Care, Germany) and blood samples were placed on 4°C and centrifuged to collect plasma. After 20 min, mice were euthanized by cervical dislocation. Quadriceps and EDL muscles were removed, immediately frozen in liquid nitrogen and stored at –80°C until further processing. Plasma ^{3}H activity was measured by scintillation counting, as previously described (5).

The muscles were pulverized and homogenized in an ice cold buffer (20mM Tris-HCl, pH 7.4, 5mM EDTA, 10 mM sodium pyrophosphate, 100 mM sodium fluorid, 2 mM sodium orthovanadate, 10 µg/µl aprotinin, 10 µg/µl leupeptin, 3 mM benzamidine, 1 mM phenylmethylsulfonyl fluoride) using a Tissue lyser (Qiagen, Maryland, USA) 1 min at 30 oscillations per second. The homogenate was divided into 3 parts: in 1) 4.5% PCA was added, in 2) 0.3 M BaOH and 0.3 M ZnSO4 were added, and in 3) 4% NP40 and 40% glycerol were added. Part 3) was placed end over end (1h 4^0C) and centrifuged (16,000g, 4^0C, 20 min) to obtain lysate for further analyses. Part 1) and 2) were centrifuged (13,000g for 4 min) and 2-[3H] deoxyglucose-6-phosphate was determined as previously described (5;6). The muscle glucose clearance calculation was based on the muscle accumulation of 2-[3H]deoxyglucose-6-phosphate activity related to the area under the curve of the plasma 3H activity at time point -2, 10 and 20 min using the trapezoid method as previously described (5;7;8). The plasma specific activity at time point 10 and 20 min was calculated by relating the plasma 3H activity to the plasma glucose concentration at these time points.

SUPPLEMENTARY DATA

LKB1 and SIK3 - kinase activity assay

LKB1 or SIK3 were immunoprecipitated (IP) from 500 μg muscle lysate with 2 μg anti-LKB1 (S611A) or 2 μg anti-SIK3 (S226B) in addition to 5 μl protein G sepharose for 2 h at 4°C. IP's were washed twice in 1 ml buffer 1 (50 mM Tris-HCl, pH 7.5, 1 mM EGTA, 1 mM EDTA, 1% Triton X-100, 1 mM sodium orthovanadate, 50 mM sodium fluoride, 5 mM sodium pyrophosphate, 0.27 M sucrose, 0.5mM PMSF and 1 mM DTT) and twice in 1 ml buffer 2 (50 mM Tris pH 7.4, 0.1 mM EGTA and 1 mM DTT). Samples were incubated at 30°C in a final volume of 50 μl (with continuous mixing) containing 50 mM HEPES pH 7.4, 10 mM $MgCl_2$, 0.1 mM EGTA, 1 mM DTT, 0.1 mM [$^{32}P\gamma$] ATP (~200-300 CPM $pmol^{-1}$) and either 0.2 mM LKBtide (LSNLYHQGKFLQT*FCGSPLYRRR) or 0.2 mM sakamototide (ALNRTSS*DSALHRRR) for 30 min. Reactions were terminated by spotting onto P81 paper and immersed in 75 mM phosphoric acid. Filters were washed 3× 10 min with phosphoric acid, rinsed briefly with acetone, air-dried and incorporated ^{32}P determined by Cherenkov counting.

AMPK - kinase activity assay

Isoform-specific AMPK activity was measured on IP's (using α1 and α2 AMPK antibodies kindly provided by Graham Hardie, University of Dundee, United Kingdom) from 200 μg of muscle lysate protein. After an overnight incubation at 4 °C, the IP was washed once in IP-buffer, once in 240 mM Hepes (pH 7.0) and 480 mM NaCl, and twice in 120 mM Hepes (pH 7.0) and 240 mM NaCl leaving 10 μl of agarose after the last wash. The reaction ran for 30 min at 30 °C in a total volume of 30 μl containing 80 mM Hepes (pH 7.0), 40 mM NaCl, 833 μM DTT, 200 μM AMP, 100 μM AMARA-peptide (Schafer-N, Denmark), 5 mM $MgCl_2$, 200 μM ATP and 2 μCi of [γ -^{33}P]-ATP (Perkin Elmer, Denmark). The reaction was stopped by adding 10 μl of 1% phosphoric acid to the reaction after which 20 μl was spotted onto P81 filter paper (Whatman, GE Healthcare, Denmark). The filter paper was afterwards washed four times 15 min in 1% phosphoric acid. The dried filter paper was analyzed for activity using a STORM scanner (Molecular Dynamics) and the specific activity was determined by using liquid scintillation (Tri-Carb 2000, Packard Instruments Co.).

Light microscopy

Quadriceps muscles from anesthetized LKB1 and WT mice (pentobarbital 6 mg $100g^{-1}$ body wt) were incubated for 5 minutes in 1g/L procain and fixed by immersion into 2% paraformaldehyde supplemented with 0.15% picric acid in 0.1M phosphate buffer during 4 hours. Twenty to thirty single muscle fibers were isolated from each muscle to perform immunostaining against mitochondria as previously described (9). For the analysis of mitochondria structural organisation, single muscle fibers were incubated over night with a polyclonal rabbit IgG anti-COXIV (Abcam, UK) diluted in buffer A (50 mM glycine, 0.25% bovine serum albumin, 0.03% saponin, and 0.05% sodium azide in PBS). Right after, fibers were washed 3 times 20 minutes in immunobuffer and, then incubated for 2 hours with goat anti rabbit IgG conjugated with Alexa Fluor 488 (Invitrogen, Denmark). After incubation with the secondary antibody, muscle fibers were washed 5 minutes in buffer A with 0.5 μg/ml of Hoechst 33342 (Invitrogen, Denmark), followed by 2 washes, 15 minutes each with buffer A and 1 last 15 minutes wash with PBS. Right after, muscle fibers were mounted with Vectashield (Vector Laboratories, Burlingame, CA). Images of the immunostained single muscle fibers were acquired with a Zeiss LSM780, through a 63x/1.40 oil DIC Plan-Apochromat objective. Hoechst was excited with a 405nm laser line, Alexa Fluor 488 was excited with a 488nm Argon laser. Imaging settings were set so that no signal was detected for the negative controls with no primary antibodies and no saturate pixels were obtained in the different conditions. Confocal z-stacks were acquired and images were processed using FiJi software.

Electron microscopy

SUPPLEMENTARY DATA

LKB1 MKO and WT mice were fixed by vascular perfusion through the left ventricle of the heart with 2% v/v glutaraldehyde in 0.05 M sodium phosphate buffer (pH 7.2) for 5 min. Quadriceps muscles (n=2) were removed and stored in the same fixative. Following isolation of suitable specimen blocks, the samples were rinsed three times in 0.15 M sodium cacodylate buffer (pH 7.2) and subsequently postfixed in 1% w/v OsO4 in 0.12 M sodium cacodylate buffer (pH 7.2) for 2 h. The specimens were dehydrated in graded series of ethanol, transferred to propylene oxide and embedded in Epon according to standard procedures. Sections, approximately 80 nm thick, were cut with a Reichert-Jung Ultracut E microtome and collected on copper grids with Formvar supporting membranes. Ultrathin sections were collected on copper grids with Formvar supporting membranes and stained with uranyl acetate and lead citrate, and subsequently examined with a Philips CM 100 TEM (Philips, Eindhoven, The Netherlands), operated at an accelerating voltage of 80 kV and equipped with an OSIS Veleta digital slow scan 2k x 2k CCD camera. A total of 15 fibers were analyzed from each muscle (n=2). All images were obtained in eucentric height for optimal comparison at x24500 magnification. Digital images were recorded with the ITEM software package.

Microarray labeling and analysis

RNA was extracted from tibialis anterior muscle from WT and LKB1 MKO mice using TRIzol. Labelling of 100 ng total RNA (100 ng) was performed using the Gene-Chip Whole Transcript Sense Target Labeling Assay (Affymetrix) followed by hybridization to the GeneChip Mouse Gene 1.0 ST Arrays (Affymetrix) according to the manufacturer's instructions. RMA16 Quantile normalization was performed in the GeneSpring 12 software package (Agilent). To filter out background noise only probe sets with raw intensity values above 100 in >2 samples were included for further analysis (18183 probes sets out of originally 28856 probe sets). Statistical analysis was performed using unpaired t-test followed by Benjamini-Hochberg multiple-testing correction. Only probe sets with a corrected p-value < 0.05 and an absolute fold change above 1.4 were selected for further analysis. Of the 212 probes sets fulfilling the criteria the gene most significantly different was Stk11 encoding for LKB1. Hierarchical clustering was done with Euclidean distance and centroid linkage. Metabolomics Pathway analysis was performed with Ingenuity Pathway Analysis (Ingenuity Systems) with the following settings: Species=Mouse, Confidence=Experimentally Observed, and Data sources=Ingenuity Expert Findings or Ingenuity Expert Assist Findings.

Protein expression and phosphorylation

Total content and phosphorylation level of proteins were determined from muscle lysates obtained as described above. Protein content was measured by the bicinchoninic acid method (Pierce) in triplicates accepting a coefficient of variation of 5%. Following SDS-PAGE, immunoblotting was performed using the following primary antibodies against total protein content: anti-LKB1 (Santa Cruz Biotechnology, CA, USA), anti-SIK3 (as previously described (10)), anti-pan α-AMPK (Cell Signaling Technology, MA, USA), anti-AMPKα2 (Kindly donated by Dr. Hardie, Dundee University), anti-ACC (Streptadivin-HRP, DAKO, Denmark), anti-SIRT1 (Cell Signaling Technology, MA, USA), anti-HDAC4 (Cell Signaling Technology, MA, USA), anti-hexokinase II (Alpha Diagnostic International INC, TX, USA), anti-GLUT4 (Thermo Scientific, MA, USA), anti-CD36 (R&D Systems, UK), anti-**β**-Actin (Sigma-Aldrich, Denmark), anti-tubulin (Sigma-Aldrich, UK), anti-FABPpm (Kindly donated by Dr. Calles-Escandon, Wake Forrest University, NC, USA), anti-FATP1 (Kindly donated by Dr. Stahl, UC Berkeley, CA, USA), anti-FATP4 (Kindly donated by Dr. Füllekrug, University of Heidelberg). Furthermore, anti-p53 and anti-acetylated p53 Lys379 (Cell Signaling Technology, MA, USA) were used. The following primary antibodies against phosphorylated proteins were applied anti-α-AMPK Thr172 phosphorylation (Cell Signaling Technology, MA, USA), anti-ACC Ser212 phosphorylation (Upstate Biotechnology Incorporated, MA, USA), and anti-HDAC4 Ser632 phosphorylation (Cell

SUPPLEMENTARY DATA

Signaling Technology, MA, USA). TBC1D1 protein expression and TBC1D1 Ser237 phosphorylation were determined after immunoprecipitation of TBC1D1, as previously described (11;12). Secondary antibodies used were all species-specific HRP-conjugated immunoglobulins (DakoCytomation, Denmark). Bands were visualized using a Kodak Image Station 2000MM (Kodak, Denmark) and an enhanced chemoluminescence system (ECL$^+$, Amersham Pharmacia Biotech, Sweden). Bands were quantified using Kodak 1D 3.6 software.

Supplementary Table 1. Blood glucose concentration and 2DG plasma specific activity during treadmill running.

	0 min	10 min	20 min
Blood glucose (mM)			
WT			
Rest	8.8±0.3	14.3±0.6*	16.5±1.2*£
Ex 60%	8.5±0.5	11.9±0.4*	13.5±0.9*£
LKB1 MKO			
Rest	7.9±0.4	12.2±0.6*	14.5±0.6*£
Ex 60%	8.7±0.4	12.5±0.7*	14.1±0.9*£
Plasma SA (dpm/µmol)			
WT			
Rest	-	80101±3927	73317±5474£
Ex 60%	-	77960±8576	67176±7253£
LKB1 MKO			
Rest	-	86592±4331	73576±4263£
Ex 60%	-	72738±5787	67176±4678£

Data are means ± SE. *, $p<0.05$; significantly different from 0 min time point. £, $p<0.05$; significantly different from 10 min time point.

SUPPLEMENTARY DATA

Supplementary Table 2. Mouse expression array analysis revealed 212 different probe sets in WT and LKB MKO muscle.

Transcripts Cluster Id	Genesymbol	Fold change	p-value (Corrected)	p-value
10364683	Stk11	-3.77	2.83E-03	8.16E-07
10427796	Npr3	2.60	2.83E-03	1.13E-06
10594517	Kbtbd13	-1.56	2.83E-03	1.20E-06
10485213	Cd82	2.53	2.83E-03	1.25E-06
10564857	Idh2	-2.13	4.99E-03	3.22E-06
10413222	Ppif	-1.61	4.99E-03	3.29E-06
10424404	Pvt1	1.79	5.04E-03	3.60E-06
10579958	Il15	-1.82	5.57E-03	4.29E-06
10574532	Ces2d-ps|Ces2c|Ces2b	1.40	6.25E-03	5.77E-06
10410984	Ckmt2	-1.71	6.25E-03	5.85E-06
10427075	Krt18	1.44	6.70E-03	6.66E-06
10465559	Vegfb	-1.48	6.70E-03	7.18E-06
10587107	Myo5a	1.78	7.60E-03	8.78E-06
10513143	Ptpn3	-1.54	7.64E-03	9.57E-06
10349711	Slc41a1	-1.77	8.19E-03	1.08E-05
10513166	Ptpn3	-1.65	9.68E-03	1.38E-05
10378857	Coro6	-1.45	1.10E-02	1.91E-05
10442445	Dci	-1.51	1.10E-02	1.96E-05
10593937	Mpi	-1.42	1.11E-02	2.23E-05
10589602	Myl3	-4.95	1.14E-02	2.38E-05
10513141	Ptpn3	-1.70	1.23E-02	2.90E-05
10354374	Slc40a1	-2.04	1.23E-02	2.93E-05
10409240	Sema4d	1.44	1.23E-02	3.24E-05
10467842	Got1	-1.48	1.32E-02	3.80E-05
10438328	D16H22S680E	-1.61	1.32E-02	3.88E-05
10589960	Gadl1	1.78	1.32E-02	3.98E-05
10587339	Gm10639|Gsta2|Gsta1|Gm3776	2.18	1.34E-02	4.48E-05
10603354	Magix	-1.44	1.34E-02	4.55E-05
10358754		1.85	1.36E-02	5.05E-05

10559694	Sbk2	1.99	1.36E-02	5.33E-05
10456254	Nedd4l	1.61	1.36E-02	5.41E-05
10544660	Osbpl3	1.62	1.36E-02	5.55E-05
10505145	Musk	2.06	1.36E-02	5.57E-05
10540105	Tmem43	1.58	1.38E-02	5.77E-05
10377662	Ybx2	-1.65	1.38E-02	5.93E-05
10359861	Mgst3	-1.66	1.40E-02	6.14E-05
10387768	Acadvl|Dvl2	-1.44	1.40E-02	6.30E-05
10439651	Cd200	-1.56	1.40E-02	6.43E-05
10404152	Fam65b	1.61	1.40E-02	6.62E-05
10483706	Chrna1	2.63	1.40E-02	6.63E-05
10441361	Tiam2|Tfb1m	2.23	1.43E-02	7.57E-05
10513145	Ptpn3	-1.74	1.44E-02	7.66E-05
10516765	Serinc2	1.64	1.61E-02	9.06E-05
10432139	Zfp641	1.45	1.67E-02	9.88E-05
10428827	Tmem65	-1.43	1.67E-02	9.91E-05
10430974	Arfgap3	1.48	1.73E-02	1.05E-04
10363455	Pcbd1	2.16	1.73E-02	1.06E-04
10361055	Vash2	1.65	1.74E-02	1.07E-04
10513158	Ptpn3	-1.85	1.77E-02	1.14E-04
10354418	Obfc2a	2.13	1.89E-02	1.31E-04
10459552	Spire1	1.40	1.89E-02	1.36E-04
10513154	Ptpn3	-1.72	1.89E-02	1.36E-04
10458046	D0H4S114	-1.80	1.90E-02	1.47E-04
10457205	Crem	1.46	1.92E-02	1.50E-04
10389300	Dhrs11	-1.46	2.05E-02	1.67E-04
10533050	Hspb8	1.54	2.06E-02	1.72E-04
10585390	Sln	2.28	2.06E-02	1.72E-04
10421648	Slc25a30	-1.48	2.06E-02	1.73E-04
10394770	Odc1	2.20	2.10E-02	1.86E-04
10538459	Aqp1	-1.66	2.10E-02	1.87E-04

SUPPLEMENTARY DATA

10456904	Pstpip2	1.50	2.10E-02	1.95E-04
10384797	Ccdc85a	-1.53	2.10E-02	1.97E-04
10541721	Spsb2	1.43	2.10E-02	2.03E-04
10468311	Sh3pxd2a	1.42	2.10E-02	2.10E-04
10598638	Mid1ip1	-1.57	2.10E-02	2.12E-04
10418053	Kcnma1	1.61	2.10E-02	2.20E-04
10605874	Eda2r	3.12	2.10E-02	2.23E-04
10431140	1810041L15Rik	1.51	2.10E-02	2.23E-04
10513156	Ptpn3	-1.72	2.15E-02	2.32E-04
10396952	Ttc9	5.34	2.15E-02	2.33E-04
10582295	Odc1	2.23	2.17E-02	2.40E-04
10506254	Raver2	-2.12	2.19E-02	2.46E-04
10552311		2.35	2.19E-02	2.48E-04
10547381	Lrtm2	1.64	2.26E-02	2.68E-04
10513139	Ptpn3	-1.69	2.26E-02	2.69E-04
10411853	Erbb2ip	1.45	2.26E-02	2.69E-04
10440513	Cyyr1	-1.42	2.26E-02	2.71E-04
10492402	Kcnab1	2.17	2.26E-02	2.71E-04
10576639	Nrp1	-1.50	2.30E-02	2.89E-04
10595148	Gsta2|Gm10639|Gsta1|Gm3776	2.20	2.30E-02	2.91E-04
10604844	Sms|Gm8234	1.63	2.30E-02	2.95E-04
10581151	Rrad	3.44	2.31E-02	2.99E-04
10603208	Mid1	1.48	2.31E-02	3.00E-04
10571444	Slc7a2	-1.46	2.31E-02	3.04E-04
10549102	Kcnj8	-1.45	2.31E-02	3.05E-04
10418011	Dupd1	1.50	2.31E-02	3.06E-04
10513162	Ptpn3	-1.81	2.31E-02	3.06E-04
10606868	Bex1	2.55	2.34E-02	3.15E-04
10564502	Pgpep1l	1.77	2.35E-02	3.17E-04
10587331	Gsta1|Gm10639|Gsta2|Gm3776	4.30	2.35E-02	3.20E-04
10462035	Ldhb	-2.55	2.36E-02	3.24E-04

SUPPLEMENTARY DATA

10607524	Sms|Gm8234	1.58	2.42E-02	3.35E-04
10451421	Klhdc3	-1.50	2.42E-02	3.40E-04
10513152	Ptpn3	-1.68	2.44E-02	3.70E-04
10553140	Tmem143	-1.42	2.44E-02	3.75E-04
10386473	Srebf1	1.69	2.47E-02	3.82E-04
10529034	Cgref1	1.78	2.48E-02	3.88E-04
10596718	Slc38a3	-1.45	2.60E-02	4.31E-04
10434815	Trp63	1.68	2.60E-02	4.34E-04
10505008	Slc44a1	1.58	2.60E-02	4.35E-04
10593293	Ncam1	3.49	2.63E-02	4.50E-04
10587323	Gsta1|Gsta2|Gm10639|Gm3776	4.67	2.64E-02	4.62E-04
10348537	Ramp1	-1.46	2.64E-02	4.64E-04
10452030	Plin3	-1.76	2.65E-02	4.70E-04
10533401	Cux2	-1.50	2.65E-02	4.71E-04
10387625	Chrnb1	1.80	2.66E-02	4.79E-04
10574023	Mt2	4.36	2.70E-02	4.93E-04
10574166	Cpne2	2.49	2.78E-02	5.27E-04
10586357	Cilp	3.05	2.78E-02	5.30E-04
10438603	Igf2bp2	1.41	2.80E-02	5.41E-04
10580635	Ces1d	-4.22	2.80E-02	5.56E-04
10463599	Nfkb2	1.44	2.80E-02	5.59E-04
10379127	Spag5	1.59	2.80E-02	5.59E-04
10524909	Nos1	-1.59	2.85E-02	5.73E-04
10370766	Gamt	2.01	2.97E-02	6.09E-04
10496359	Emcn	-1.44	2.99E-02	6.22E-04
10376201	Gpx3	-1.94	2.99E-02	6.25E-04
10387909	Chrne	1.49	2.99E-02	6.25E-04
10403076		1.72	2.99E-02	6.29E-04
10413086	Adk	-1.51	3.06E-02	6.60E-04
10465089	Snx32	1.49	3.10E-02	6.77E-04
10408600	Serpinb6a	1.50	3.12E-02	6.86E-04

10529895	Qdpr	1.46	3.14E-02	7.01E-04
10484307	Frzb	-1.76	3.15E-02	7.19E-04
10355567	Tmbim1	1.44	3.15E-02	7.21E-04
10517609	Cda	-1.44	3.17E-02	7.37E-04
10536494	Cav2	-1.47	3.17E-02	7.40E-04
10447773	Slc22a3	2.57	3.17E-02	7.46E-04
10584317	Esam	-1.41	3.17E-02	7.49E-04
10513160	Ptpn3	-1.82	3.17E-02	7.70E-04
10556302	Ampd3	1.41	3.17E-02	7.75E-04
10590983	Panx1	1.74	3.21E-02	7.90E-04
10471844	Nek6	1.50	3.35E-02	8.38E-04
10519983	Fgl2	1.87	3.35E-02	8.39E-04
10528207	Cd36	-1.47	3.37E-02	8.46E-04
10445268	Gpr116	-1.41	3.38E-02	8.53E-04
10472923	Ak4	-2.36	3.40E-02	8.68E-04
10575993	6430548M08Rik	1.65	3.43E-02	8.85E-04
10549097	Ldhb	-1.94	3.43E-02	8.87E-04
10412909	Fdft1	-1.41	3.45E-02	8.94E-04
10463355	Scd2	2.31	3.45E-02	8.99E-04
10513164	Ptpn3	-1.83	3.46E-02	9.05E-04
10447317	Epas1	-1.51	3.47E-02	9.17E-04
10399228		1.65	3.49E-02	9.24E-04
10456400	Tubb6	2.35	3.49E-02	9.25E-04
10473022	Plp2	1.72	3.65E-02	9.94E-04
10394109	Rab40b	1.44	3.65E-02	1.00E-03
10417869	Anxa7	1.57	3.65E-02	1.01E-03
10441680	Pde10a	1.63	3.66E-02	1.02E-03
10577782	Htra4	3.03	3.66E-02	1.03E-03
10491825	3110057O12Rik	-1.56	3.66E-02	1.03E-03
10346164	Sdpr	-1.45	3.74E-02	1.06E-03
10443463	Cdkn1a	2.68	3.74E-02	1.09E-03

SUPPLEMENTARY DATA

10500283	Car14|Aph1a	-1.89	3.78E-02	1.11E-03
10377245	Dhrs7c	-1.54	3.78E-02	1.12E-03
10359689	Atp1b1	-1.48	3.79E-02	1.12E-03
10411519	Mtap1b	2.12	3.80E-02	1.14E-03
10379190	Vtn	-1.44	3.87E-02	1.19E-03
10471247	Aif1l	1.52	3.88E-02	1.19E-03
10407420	Net1	1.41	3.88E-02	1.20E-03
10607089	Acsl4	1.46	3.88E-02	1.21E-03
10371502	Fabp3	-1.50	3.88E-02	1.22E-03
10355246	Acadl	-1.45	3.88E-02	1.23E-03
10502590	Clca6	1.45	3.88E-02	1.24E-03
10540952	Ift122	1.47	3.89E-02	1.26E-03
10411359	Plp2|Prickle3	1.68	3.90E-02	1.28E-03
10475625	Eid1	1.47	3.90E-02	1.28E-03
10583242	Sesn3	1.57	3.93E-02	1.31E-03
10545401	Vamp5	-1.47	3.96E-02	1.35E-03
10559796	Peg3	1.91	3.98E-02	1.36E-03
10366153	Rassf9	-1.43	3.98E-02	1.37E-03
10543306	Tspan12	-1.48	4.00E-02	1.38E-03
10490159	Pmepa1	1.54	4.04E-02	1.40E-03
10508614	Fabp3	-1.51	4.04E-02	1.40E-03
10588495	Dusp7	-1.84	4.15E-02	1.46E-03
10603346	Plp2|Prickle3	1.68	4.21E-02	1.52E-03
10451953	Lrg1	-1.66	4.21E-02	1.52E-03
10380285	Tmem100	3.22	4.23E-02	1.53E-03
10392347	Pitpnc1	-1.46	4.33E-02	1.58E-03
10542791	Ppfibp1	1.43	4.34E-02	1.59E-03
10355536	Tns1	-1.49	4.37E-02	1.62E-03
10548532	Klra9|Klra5|Klra3	-1.52	4.37E-02	1.63E-03
10402117	Rps6ka5	-1.76	4.43E-02	1.66E-03
10397763	9030617O03Rik	-1.80	4.44E-02	1.67E-03

10344973	Gdap1	2.18	4.46E-02	1.69E-03
10362959	Popdc3	1.55	4.47E-02	1.70E-03
10367591	Myct1	-1.48	4.49E-02	1.72E-03
10374998	Gpr75	1.77	4.50E-02	1.73E-03
10591620	Dock6	-1.42	4.50E-02	1.73E-03
10495285	Sort1	1.43	4.59E-02	1.80E-03
10502375	Mttp	1.41	4.60E-02	1.82E-03
10533483	Atp2a2	1.53	4.61E-02	1.83E-03
10572130	Lpl	-1.42	4.64E-02	1.85E-03
10535807	Flt1	-1.44	4.68E-02	1.89E-03
10591630	Dock6	-1.41	4.68E-02	1.90E-03
10475437	Sord	-1.47	4.69E-02	1.91E-03
10521678	Cd38	-1.45	4.69E-02	1.92E-03
10494889	Dennd2c	1.94	4.69E-02	1.93E-03
10347748	Acsl3|Utp14b	1.55	4.69E-02	1.93E-03
10491820	3110057O12Rik|Gm2011	-1.40	4.73E-02	1.97E-03
10424221	Wdr67	1.65	4.73E-02	1.97E-03
10533849	Rilpl1	-1.50	4.76E-02	2.00E-03
10536898	Irf5	-1.68	4.76E-02	2.01E-03
10441003	Runx1	2.48	4.77E-02	2.02E-03
10555118	Pak1	1.62	4.81E-02	2.05E-03
10490923	Car2	-1.62	4.82E-02	2.06E-03
10499899	Sprr1a	1.47	4.83E-02	2.08E-03
10505030	Fsd1l	1.64	4.87E-02	2.12E-03
10467191	Ankrd1	5.68	4.90E-02	2.15E-03
10545672	Mthfd2	1.91	4.94E-02	2.17E-03
10530536	Tec	1.56	4.94E-02	2.17E-03
10522208	Uchl1	2.11	4.99E-02	2.20E-03

SUPPLEMENTARY DATA

Supplementary Table 3. Mouse expression array analysis revealed differences in 27 genes involved lipid metabolism.

Transcripts Cluster Id	Gene symbol	Gene name	Fold change	p-value (Corrected)	p-value
10364683	Stk11	serine/threonine kinase 11 (LKB1)	-3.77	2.83E-03	8.16E-07
10579958	Il15	interleukin 15	-1.82	5.57E-03	4.29E-06
10587107	Myo5a	myosin VA	1.78	7.60E-03	8.78E-06
10442445	Dci	enoyl-CoA delta isomerase 1	-1.51	1.10E-02	1.96E-05
10467842	Got1	glutamate oxaloacetate transaminase 1	-1.48	1.32E-02	3.80E-05
10456254	Nedd4l	neural precursor cell expressed, developmentally down-regulated gene 4-like	1.61	1.36E-02	5.41E-05
10387768	Acadvl	acyl-Coenzyme A dehydrogenase, very long chain	-1.44	1.40E-02	6.30E-05
10457205	Crem	cAMP responsive element modulator	1.46	1.92E-02	1.50E-04
10598638	Mid1ip1	mid1 interacting protein 1	-1.57	2.10E-02	2.12E-04
10418053	Kcnma1	potassium large conductance calcium-activated channel, subfamily M, alpha member 1	1.61	2.10E-02	2.20E-04
10581151	Rrad	Ras-related associated with diabetes	3.44	2.31E-02	2.99E-04
10386473	Srebf1	sterol regulatory element binding transcription factor 1	1.69	2.47E-02	3.82E-04
10574023	Mt2	metallothionein 2	4.36	2.70E-02	4.93E-04
10580635	Ces1d	carboxylesterase 1D	-4.22	2.80E-02	5.56E-04
10524909	Nos1	nitric oxide synthase 1, neuronal	-1.59	2.85E-02	5.73E-04
10528207	Cd36	CD36 antigen	-1.47	3.37E-02	8.46E-04
10412909	Fdft1	farnesyl diphosphate farnesyl transferase 1	-1.41	3.45E-02	8.94E-04
10463355	Scd2	stearoyl-Coenzyme A desaturase 2	2.31	3.45E-02	8.99E-04
10447317	Epas1	endothelial PAS domain protein 1	-1.51	3.47E-02	9.17E-04
10443463	Cdkn1a	cyclin-dependent kinase inhibitor 1A (P21)	2.68	3.74E-02	1.09E-03
10607089	Acsl4	acyl-CoA synthetase long-chain family member 4	1.46	3.88E-02	1.21E-03
10355246	Acadl	acyl-Coenzyme A dehydrogenase, long-chain	-1.45	3.88E-02	1.23E-03
10508614	Fabp3	fatty acid binding protein 3, muscle and heart	-1.51	4.04E-02	1.40E-03
10502375	Mttp	microsomal triglyceride transfer protein	1.41	4.60E-02	1.82E-03
10533483	Atp2a2	ATPase, Ca++ transporting, cardiac muscle, slow twitch 2	1.53	4.61E-02	1.83E-03
10572130	Lpl	lipoprotein lipase	-1.42	4.64E-02	1.85E-03
10521678	Cd38	CD38 antigen	-1.45	4.69E-02	1.92E-03

SUPPLEMENTARY DATA

Supplementary Figure 1. LKB1 MKO mice are AICAR intolerant. Mice were injected intraperitoneally with AICAR (0.5 g/kg body weight) and blood drawn from the tail vein was used for blood glucose measurement (n=18-23). Experiments were performed blinded and in randomized order. **, p<0.01; significantly different from WT. Data are presented as means ± SEM.

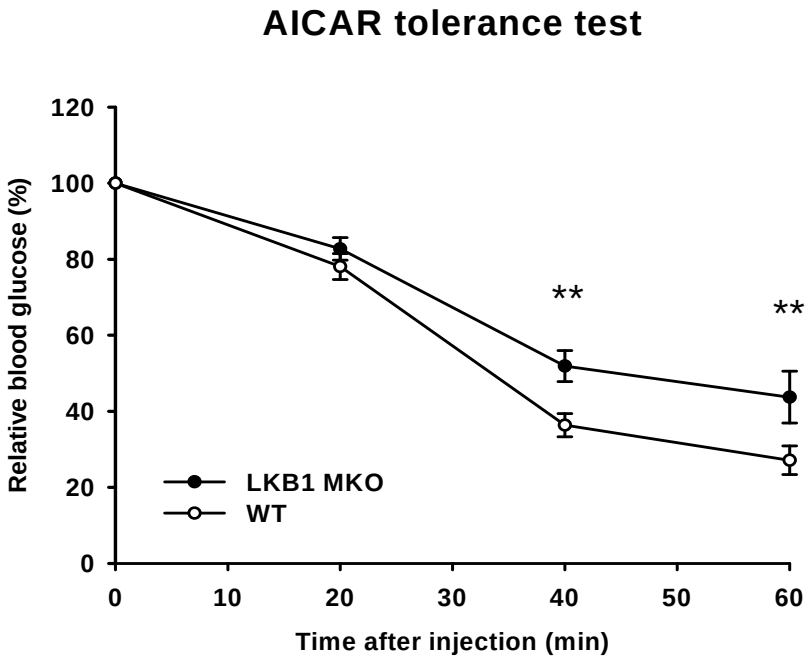

Supplementary Figure 2. LKB1 MKO has normal resting oxygen uptake and RER under fed conditions. At rest LKB1 MKO and WT mice had similar A) oxygen uptake and B) RER both at night and during light periods determined by indirect calorimetry. Data are presented as means ± SEM (n=8).

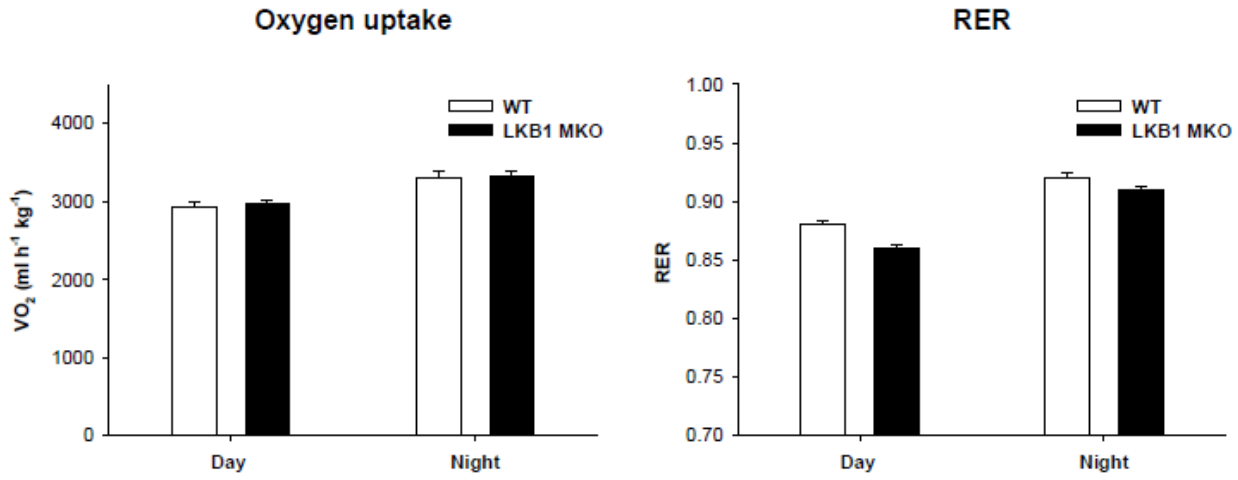

SUPPLEMENTARY DATA

Supplementary Figure 3. AMPKα2 KO mice have reduced oxygen uptake, but normal RER and fat oxidation during exercise. A) Exercise capacity test were performed by treadmill running, where maximum speed was the cut-off speed found by increasing running speed by 2.4 m/min every 2nd minute until exhaustion. AMPKα2 KO mice had a reduced treadmill running speed capacity compared to WT littermates. B) AMPK α2 KO mice displayed normal RER, but C) lower oxygen uptake (ml h^{-1} kg^{-1}), determined by indirect calorimetry during the last 18 min of a 36 min exercise bout at the same relative intensity (50% of max running speed). D-E) During the last 18 min of a 36 min exercise bout whole body carbohydrate- and fat oxidation (kJ h^{-1} kg^{-1}) was similar between genotypes. Data are presented as means ± SEM (n=8). **/***, p<0.01/p<0.001; significantly different from WT.

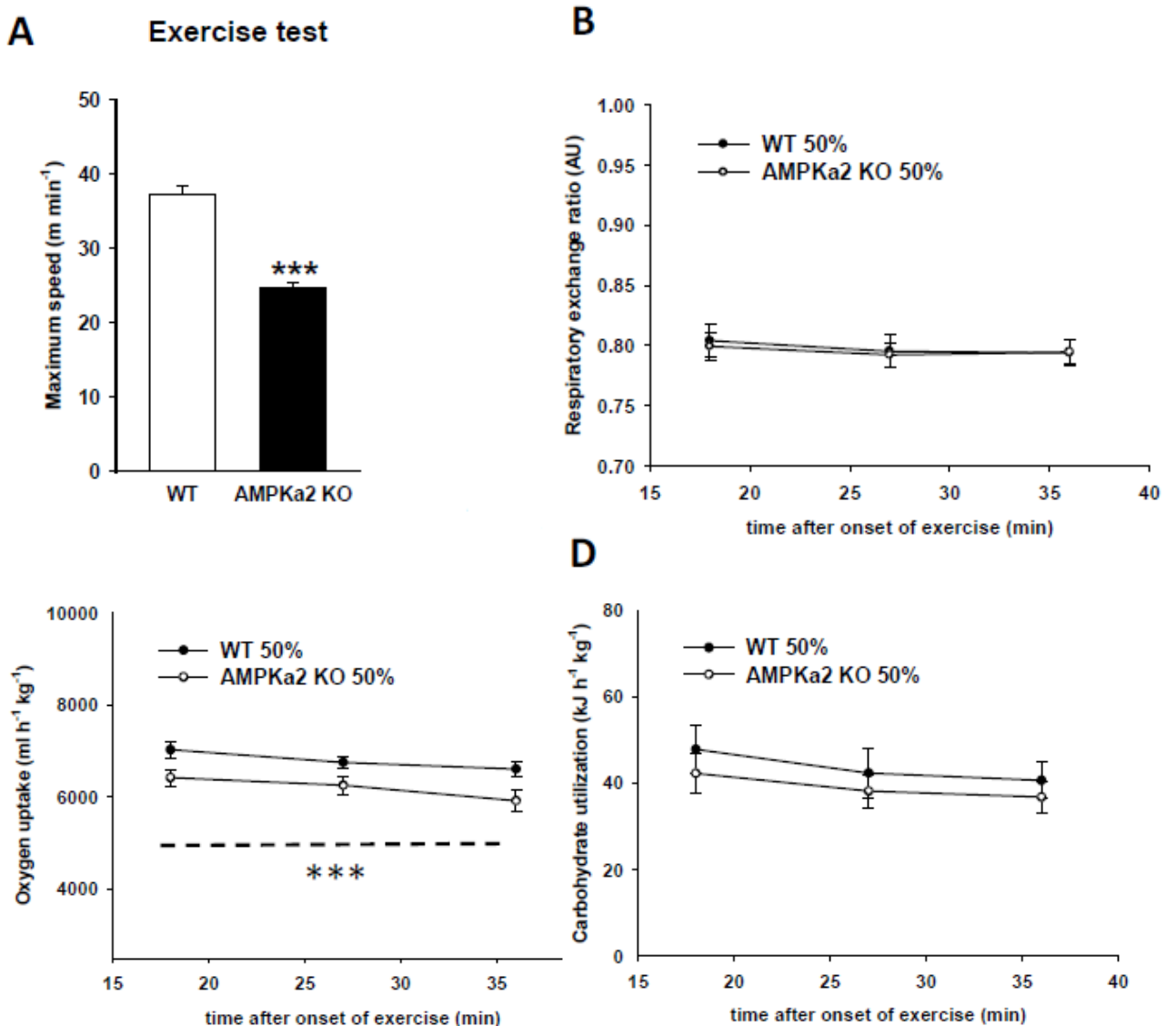

SUPPLEMENTARY DATA

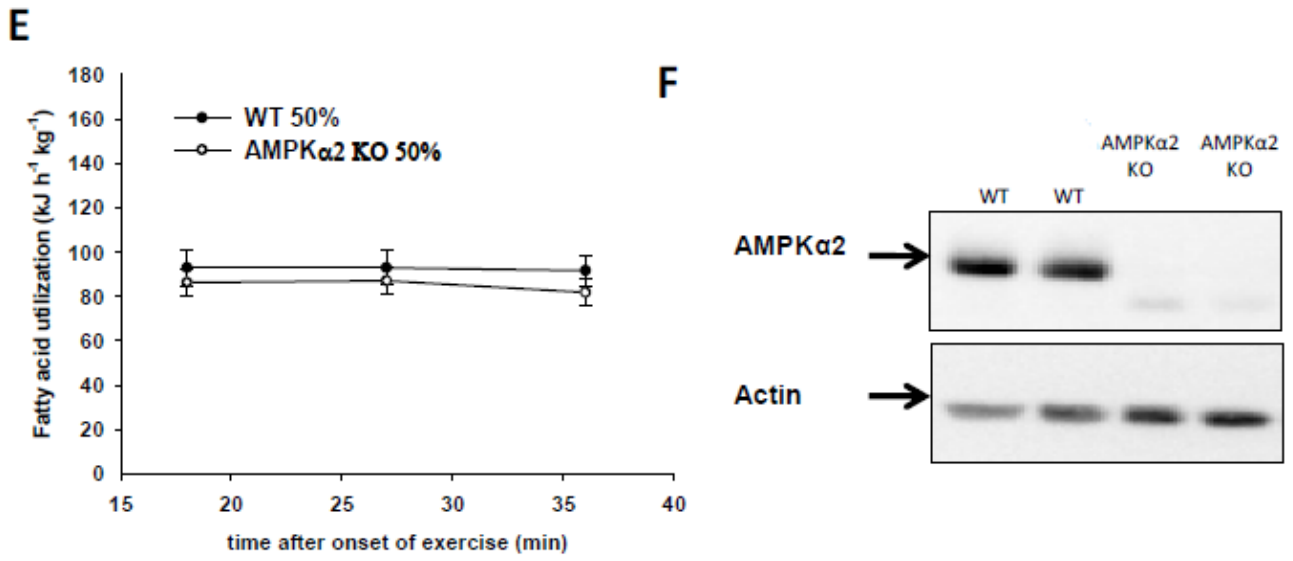

Supplementary Figure 4. Nucleotide levels in LKB1 MKO and WT muscle at rest and after exercise. There was no difference in resting muscle nucleotide levels between WT and LKB1 MKO mice. Furthermore, AMP:ATP and ADP:ATP ratios increased with exercise to a similar extent in both genotypes. Data are presented as means ± SEM (n=7-10).

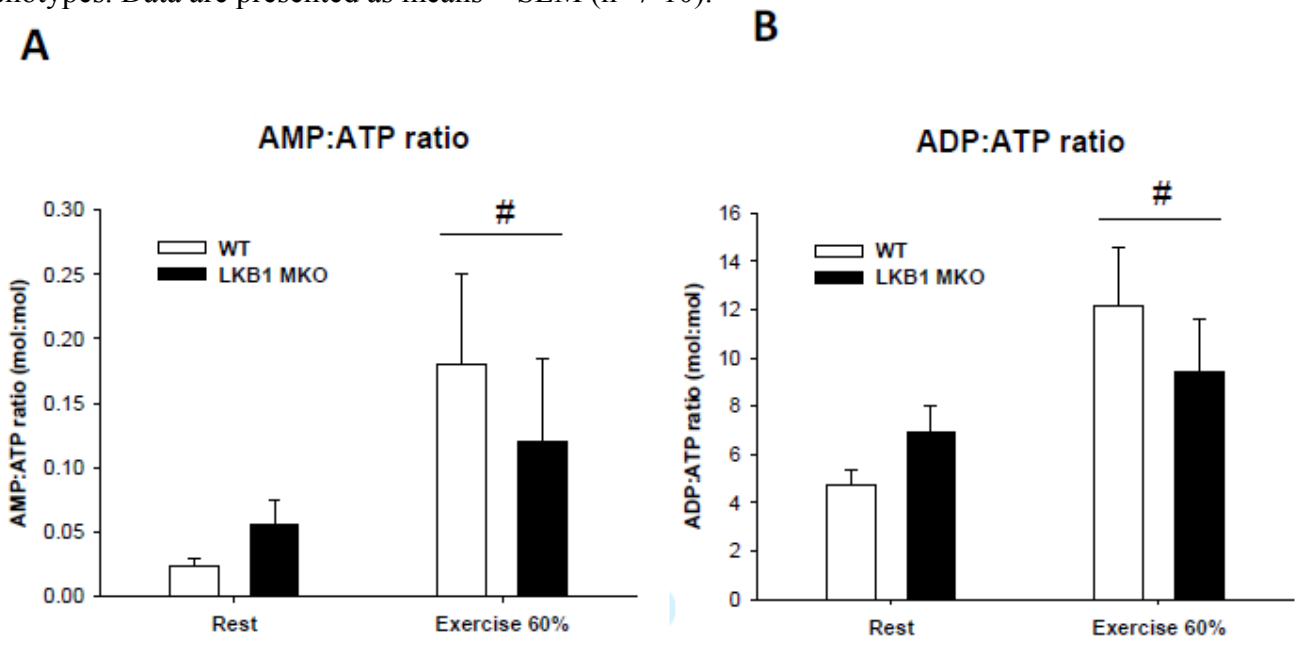

SUPPLEMENTARY DATA

Supplementary Figure 5. Lipid binding proteins, GLUT4 and HKII expression in muscle lacking LKB1 protein. The lipid binding proteins A) fatty acid translocase CD36 (FAT/CD36) and C-D) fatty acid transport protein 1 and 4 were equally expressed in quadriceps muscle from WT and LKB1 MKO mice, whereas the B) membrane bound fatty acid binding protein (FABPpm) was reduced in LKB1 MKO muscle (n=7-13). E) Glucose transporter 4 (GLUT4) was higher in quadriceps muscle from LKB1 MKO mice (n=23-28), whereas hexokinase II protein expression (HKII) was similarly expressed in quadriceps muscle from WT and LKB1 MKO mice (n=23-28). Data are presented as means ± SEM. *, $p<0.05$; significantly different from WT.

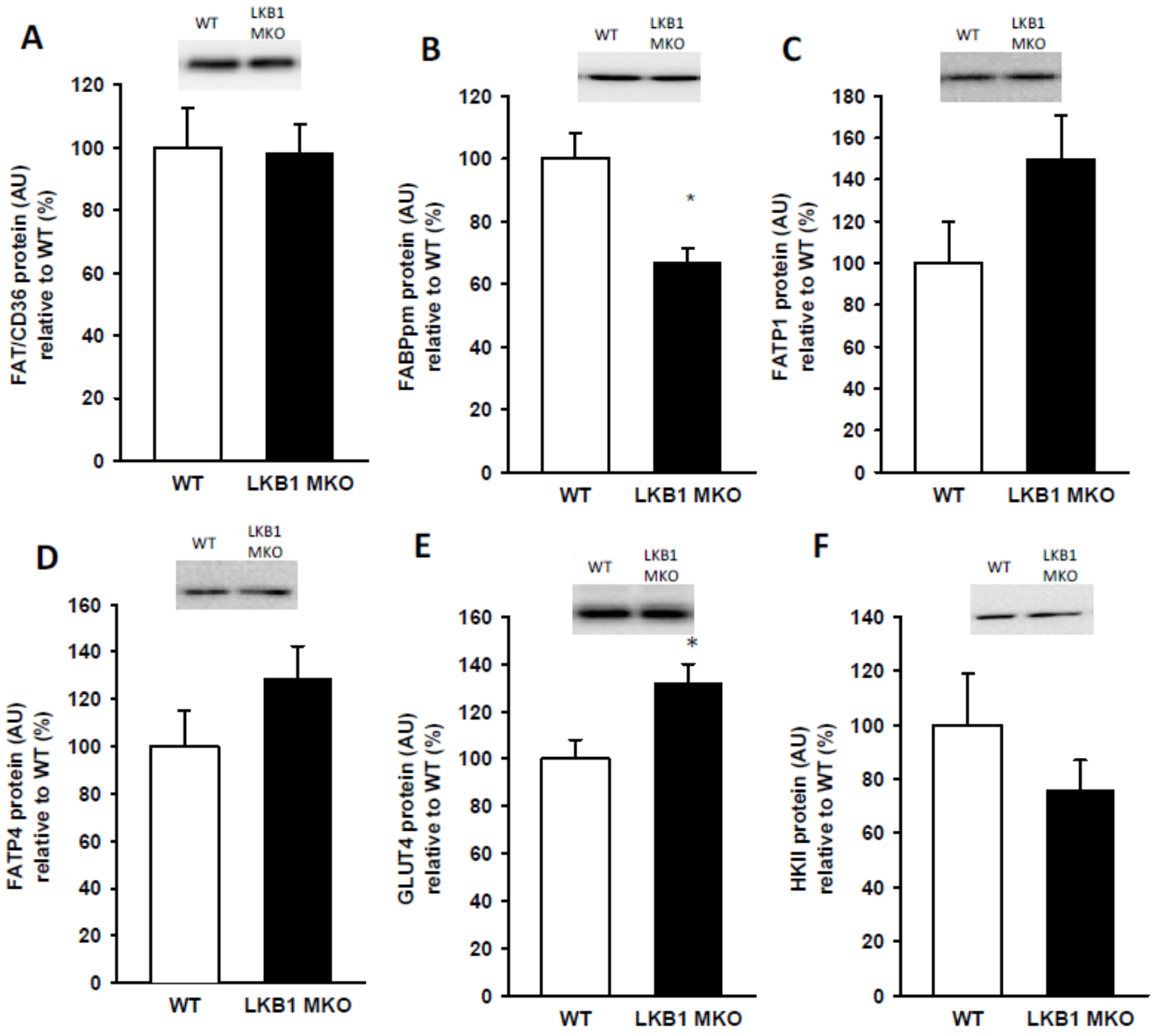

SUPPLEMENTARY DATA

Reference List

1. Steinberg,GR, Bonen,A, Dyck,DJ: Fatty acid oxidation and triacylglycerol hydrolysis are enhanced after chronic leptin treatment in rats. *Am J Physiol Endocrinol Metab* 282:E593-E600, 2002
2. Dzamko,N, Schertzer,JD, Ryall,JG, Steel,R, Macaulay,SL, Wee,S, Chen,ZP, Michell,BJ, Oakhill,JS, Watt,MJ, Jorgensen,SB, Lynch,GS, Kemp,BE, Steinberg,GR: AMPK-independent pathways regulate skeletal muscle fatty acid oxidation. *J Physiol* 586:5819-5831, 2008
3. Jorgensen,SB, Viollet,B, Andreelli,F, Frosig,C, Birk,JB, Schjerling,P, Vaulont,S, Richter,EA, Wojtaszewski,JF: Knockout of the alpha2 but not alpha1 5'-AMP-activated protein kinase isoform abolishes 5-aminoimidazole-4-carboxamide-1-beta-4-ribofuranosidebut not contraction-induced glucose uptake in skeletal muscle. *J Biol Chem* 279:1070-1079, 2004
4. Koh,HJ, Toyoda,T, Fujii,N, Jung,MM, Rathod,A, Middelbeek,RJ, Lessard,SJ, Treebak,JT, Tsuchihara,K, Esumi,H, Richter,EA, Wojtaszewski,JF, Hirshman,MF, Goodyear,LJ: Sucrose nonfermenting AMPK-related kinase (SNARK) mediates contraction-stimulated glucose transport in mouse skeletal muscle. *Proc Natl Acad Sci U S A* 107:15541-15546, 2010
5. Maarbjerg,SJ, Jorgensen,SB, Rose,AJ, Jeppesen,J, Jensen,TE, Treebak,JT, Birk,JB, Schjerling,P, Wojtaszewski,JF, Richter,EA: Genetic impairment of {alpha}2-AMPK signaling does not reduce muscle glucose uptake during treadmill exercise in mice. *Am J Physiol Endocrinol Metab* 297:E924-E934, 2009
6. Ferre,P, Leturque,A, Burnol,AF, Penicaud,L, Girard,J: A method to quantify glucose utilization in vivo in skeletal muscle and white adipose tissue of the anaesthetized rat. *Biochem J* 228:103-110, 1985
7. Fueger,PT, Bracy,DP, Malabanan,CM, Pencek,RR, Wasserman,DH: Distributed control of glucose uptake by working muscles of conscious mice: roles of transport and phosphorylation. *Am J Physiol Endocrinol Metab* 286:E77-E84, 2004
8. Kraegen,EW, James,DE, Jenkins,AB, Chisholm,DJ: Dose-response curves for in vivo insulin sensitivity in individual tissues in rats. *Am J Physiol* 248:E353-E362, 1985
9. Ploug,T, van,DB, Ai,H, Cushman,SW, Ralston,E: Analysis of GLUT4 distribution in whole skeletal muscle fibers: identification of distinct storage compartments that are recruited by insulin and muscle contractions. *J Cell Biol* 142:1429-1446, 1998
10. Sakamoto,K, Goransson,O, Hardie,DG, Alessi,DR: Activity of LKB1 and AMPK-related kinases in skeletal muscle: effects of contraction, phenformin, and AICAR. *Am J Physiol Endocrinol Metab* 287:E310-E317, 2004
11. Pehmoller,C, Treebak,JT, Birk,JB, Chen,S, Mackintosh,C, Hardie,DG, Richter,EA, Wojtaszewski,JF: Genetic disruption of AMPK signaling abolishes both contraction- and insulin-stimulated TBC1D1 phosphorylation and 14-3-3 binding in mouse skeletal muscle. *Am J Physiol Endocrinol Metab* 297:E665-E675, 2009
12. Chen,S, Murphy,J, Toth,R, Campbell,DG, Morrice,NA, Mackintosh,C: Complementary regulation of TBC1D1 and AS160 by growth factors, insulin and AMPK activators. *Biochem J* 409:449-459, 2008